

Cascade Control of PM DC Drives Via Second-Order Sliding-Mode Technique

Alessandro Pisano, *Member, IEEE*, Alejandro Davila, Leonid Fridman, *Member, IEEE*, and Elio Usai, *Member, IEEE*

Abstract—This paper presents a novel scheme for the speed/position control of permanent-magnet (PM) dc motor drives. A cascade-control scheme, based on multiple instances of a second-order sliding-mode-control (2-SMC) algorithm, is suggested, which provides accurate tracking performance under large uncertainty about the motor and load parameters. The overall control scheme is composed of three main blocks: 1) a 2-SMC-based velocity observer which uses only position measurements; 2) a 2-SMC-based velocity control loop that provides a reference command current; and 3) a 2-SMC-based current control loop generating the reference voltage. The proposed scheme has been implemented and tested experimentally on a commercial PM dc motor drive. The experimental results confirm the precise and robust performance and the ease of tuning and implementation, featured by the proposed scheme.

Index Terms—Cascade control, dc motor drives, second-order sliding-mode (2-SM) control (2-SMC), SM differentiators.

I. INTRODUCTION

THE CONVENTIONAL linear control-system design for permanent-magnet (PM) dc motor drives consists of a properly tuned cascade configuration of PI speed and torque controllers. Rather accurate information regarding the motor parameters and load conditions is necessary to guarantee the desired tradeoff between precision, bandwidth, and disturbance rejection [1]. Unfortunately, several electromechanical parameters are not exactly known and/or subject to large variations during operation, leading to degradation of the drive performance.

To overcome this drawback, several “robust” control techniques have been suggested to cope with the uncertainty con-

ditions, ranging from adaptive and H_∞ control, integrator backstepping, neural networks based, and proper combinations of them [2]–[6].

Besides the earlier methods, a widely and successfully applied nonlinear control approach for controlling electrical drives is the variable-structure-control (VSC) method [7]–[10]. Such an approach has been widely applied to control dc motors, as well as other types of asynchronous and synchronous machines, and also power converters [8], [11]–[13]. In [14], VSC techniques are applied to very high precision motion control with a piezostage.

Generally speaking, the main features of VSC are high accuracy, simplicity (of both tuning and implementation) [15], and robustness [8].

VSC schemes are typically based on control signals of the switching type, and the so-called “chattering” phenomenon, originated by the interaction between parasitic dynamics and high-frequency switching control, arises, which represents the most deleterious implementation drawback of VSC [8], [10], [12]. The most common approach to alleviate the effect of chattering is the so-called “boundary-layer” control [16], [17], in which the sign function is replaced by some smooth approximation inside a suitable, possibly time varying, boundary layer of the switching surface. The following works [8], [11], [15]–[17], and references therein, can be cited as examples of continuous and discrete-time nonlinear robust techniques for PM dc drives. Although VSC schemes, also including some of the cited references, often use the boundary-layer control approach, this method is not completely satisfactory. Indeed, it solves the problem only partially, particularly when high dynamic performance are required [10], since the main characteristics of invariance and accuracy of VSC systems are not assured any more.

In order to counteract the chattering phenomenon and to preserve at the same time the main advantages of the original approach (precision, robustness, simplicity, and finite-time convergence) even when stringent dynamic specifications are met for the closed-loop system, the features of the second-order sliding-mode-control (2-SMC) technique [18]–[23] are exploited in this paper to design a cascade-based architecture represented by the block scheme shown in Fig. 1 (the meaning of the signals shown in Fig. 1 will be explained throughout this paper).

The task is to make the speed error $\omega_r - \hat{\omega}$ to tend as close as possible to zero. In Fig. 1, it can be identified the external 2-SMC velocity loop, the internal 2-SMC current loop, the velocity observer (2-SM differentiator), and a proper low-pass “smoothing filter” (a linear first-order filter).

Manuscript received January 23, 2008; revised July 8, 2008. First published August 15, 2008; current version published October 31, 2008. This work was supported by the 2007–2009 Italia–Mexico Executive Cooperation Program under Grant SAPP-8. The work of A. Pisano and E. Usai was supported by the European Community STREP FP7 Project “Prodi” under Grant 224233. The work of L. Fridman and A. Davila was supported in part by the Mexican Consejo Nacional de Ciencia y Tecnologia (CONACyT) under Grant 56819 and Fellowship 208168, in part by the Programa de Apoyo a Proyectos de Investigacion e Innovacion Tecnologica (PAPIIT) UNAM under Grant IN111208, and in part by the Programa de Apoyo a Proyectos para la Innovacion y Mejoramiento de la Enseñanza (PAPIME) UNAM under Grant PE100907.

A. Pisano and E. Usai are with the Department of Electrical and Electronic Engineering, University of Cagliari, 09123 Cagliari, Italy (e-mail: pisano@diee.unica.it; eusai@diee.unica.it).

A. Davila and L. Fridman are with the Department of Control, Division of Electrical Engineering of Engineering Faculty, National Autonomous University of Mexico, Mexico City 04510, Mexico (e-mail: alets_davila@hotmail.com; lfridman@servidor.unam.mx).

Color versions of one or more of the figures in this paper are available online at <http://ieeexplore.ieee.org>.

Digital Object Identifier 10.1109/TIE.2008.2002715

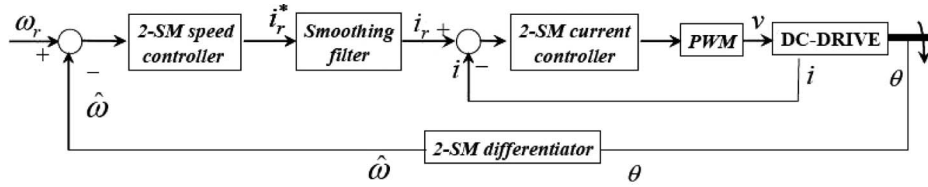


Fig. 1. Block scheme of the proposed cascade controller.

The suggested 2-SM differentiator was thoroughly discussed in [21], with specific relevance to the digital differentiation of incremental encoder measurements, which is the case of interest in this paper.

The reason for introducing the smoothing filter is that, from the convergence analysis of the internal current loop, it is concluded that it can only accept a reference input i_r having bounded first and second derivatives. Since the signal i_r^* has a discontinuous time derivative, a first-order filter can perform the required smoothing action. In the stability analysis of the overall closed-loop system in Fig. 1, the smoothing filter is treated as a fast parasitic dynamics, and the analysis developed in [22] are exploited to prove that the speed- and current-error variables both tend to a small residual set. The discrete-time implementation of the scheme is detailed along this paper; the dependence of the tracking accuracy from the sampling period and measurement noise magnitudes is investigated; and a criterion for selecting the time constant of the smoothing filter depending on the adopted sampling period is given.

Some related recent contributions are [24]–[26]. In all of them, there is a “single-loop” controller configuration without the current feedback loop. In [24], the estimation of the shaft velocity was required, similarly to the scheme we are going to outline in this paper. In [25], a different structure for the velocity loop was considered such that the estimation of both the shaft velocity and *acceleration* was actually required. A higher order SM differentiator [27] was considered to provide the required estimates.

The main difference between the approaches in [24] and [25] is that, in [24], the control voltage is given as a high-frequency switching discontinuous signal; thus, such “logical” control signal was used to directly drive the legs of the switching converter (in other words, no pulsewidth-modulation (PWM) block is needed). In [25], however, the control voltage is produced as a continuous reference which needs to be pulsewidth modulated. The approach proposed in this paper, as well as the scheme in [26], belong to the second category, i.e., they both require the PWM of a continuous voltage reference signal. In [26], a structure similar to that in [25], but using a different 2-SM algorithm, was proposed. An obvious weak point of [25] is represented by the need for estimating the shaft acceleration. As shown in Fig. 1, in this paper, we dispense with the requirement for acceleration estimation. The measurement of the current, which can be made by cheap and reliable electronic devices, is well suited for practical implementation.

The structure of this paper is as follows. Section II contains the system model formulation and the statement of the control problem, including the main standing assumptions. Section III details the proposed observer/controller structure.

Section IV discusses the main implementation issues and presents the discrete-time version of the proposed scheme; Section V presents some experimental results; and Section VI gives some concluding remarks.

II. PROBLEM FORMULATION

The PM dc-motor dynamics can be well approximated by the following linear time-invariant (LTI) state equation:

$$\begin{cases} J \frac{d}{dt} \omega(t) = -b\omega(t) + k_t i(t) - T_L(t) \\ l \frac{d}{dt} i(t) = -ri(t) - k_e \omega(t) + v(t) \end{cases} \quad (1)$$

where $\omega(t)$ is the shaft speed, $i(t)$ is the motor current, $v(t)$ is the supply voltage, $T_L(t)$ is the load torque, J and b are the overall mechanical inertia and the viscous friction coefficient at the motor shaft, respectively, k_t is the torque constant, l and r are the armature inductance and resistance, respectively, and k_e is the back electromagnetic-force constant. All motor parameters are assumed uncertain. The knowledge of some limit values for the system parameters and variables is met according to the following items.

- 1) There are known positive constants $\underline{J}, \bar{J}, \dots, \bar{k}_e$ such that the following inequalities hold:

$$\begin{aligned} \underline{J} \leq J \leq \bar{J}, \quad \underline{b} < b \leq \bar{b}, \quad \underline{k}_t \leq k_t \leq \bar{k}_t \\ \underline{l} \leq l \leq \bar{l}, \quad \underline{r} \leq r \leq \bar{r}, \quad \underline{k}_e \leq k_e \leq \bar{k}_e. \end{aligned} \quad (2)$$

- 2) The load torque satisfies the following restrictions for some known constants \bar{T}_L, \bar{T}_{L_d} :

$$|T_L| \leq \bar{T}_L \quad |\dot{T}_L| \leq \bar{T}_{L_d}. \quad (3)$$

- 3) There are two known constants Ω_d and I_d such that

$$\left| \frac{d}{dt} \omega \right| \leq \Omega_d \quad (4)$$

$$\left| \frac{d}{dt} i(t) \right| \leq I_d. \quad (5)$$

Under the physical constraint of bounded supply voltage and load torque, (4) and (5) could be derived by exploiting the input-to-state stability of the linear asymptotically stable dc-motor dynamics.

The shaft position θ and motor current i are available for measurement, while the shaft speed ω is assumed to be unknown. Consider a bounded and smoothed velocity profile

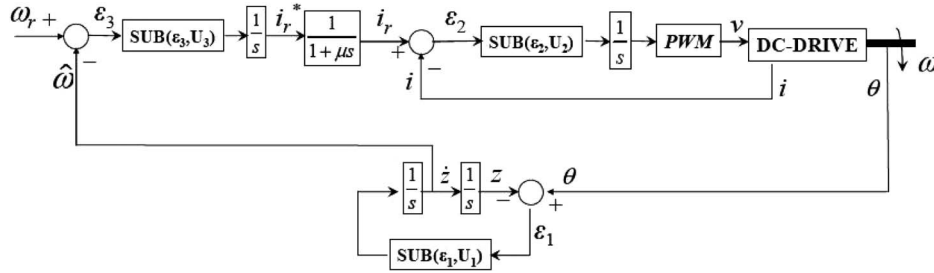


Fig. 2. Detailed representation of the proposed control system.

ω_r fulfilling the following condition for some known design constant Ω_{rdd} :

$$|\ddot{\omega}_r| \leq \Omega_{\text{rdd}}. \quad (6)$$

The control task is to define a continuous chattering-free voltage profile $v(t)$ guaranteeing the finite-time convergence of the speed-tracking error $\omega - \omega_r$ to a small vicinity of zero in spite of the parameter uncertainties, external perturbations, and measurement errors.

Remark 1: For position-control purposes, the reference speed ω_r should be set as follows:

$$\omega_r = \dot{\theta}_r + c(\theta_r - \theta), \quad c > 0 \quad (7)$$

where θ_r is a sufficiently smooth shaft-position desired profile fulfilling the condition $|\theta_r^{(3)}| \leq \Omega_{\text{rdd}}$. The required smoothing conditions on the position/velocity references seem to exclude commonly used reference signals such as square or triangular waves. It should be noted that those stringent restrictions are of mostly theoretical nature, since they serve to guarantee the possibility of achieving perfect tracking which is clearly impossible to achieve when using, for instance, a discontinuous square-wave reference for either the shaft position or velocity. In any case, the use of discontinuous references should be avoided, and smoothed references should be preferred. This topic is investigated in the experimental tests discussed in Section V (see, in particular, TEST 3 versus TEST 4).

III. CONTROL-SYSTEM DESIGN

According to a common practice in dc-drive control-system design, the cascade-control structure shown in Fig. 1, having two separate speed and current control loops, is employed (a more detailed representation of the proposed control system is shown in Fig. 2).

The velocity observer, located in the feedback loop, is a real-time robust differentiator based on the 2-SMC technique [21] that computes the first derivative of the position measurement θ and provides a *finite-time-converging* velocity estimate $\hat{\omega}$. It contains a block labeled “SUB” that represents the discontinuous “suboptimal” 2-SMC algorithm [19].

The outer loop 2-SM speed controller (containing another instance of suboptimal algorithm plus an integrator) processes the speed error $\varepsilon_3 = \omega_r - \hat{\omega}$ and is followed by a linear first-order filter. The filter output i_r^* is the command current that

feeds the inner current loop which produces the voltage profile v to be applied to the drive via classical PWM.

The 2-SMC speed and current controllers, as well as the velocity observer, are based on three different instances of the “suboptimal” controller which is denoted generically as $\text{SUB}(x(t), W)$ [19]. Define the discontinuous function $\text{SUB}(x(t), W)$ as follows:

$$\text{SUB}(x(t), W) = -W \text{sign} \left(x(t) - \frac{1}{2} x_M(t) \right) \quad (8)$$

where W is a constant positive tuning parameter, $x(t)$ is a scalar signal, and signal $x_M(t)$ is defined as

$$x_M(t) = \begin{cases} x(0), & 0 \leq t < t_{M_1} \\ x(t_{M_i}), & t_{M_i} \leq t < t_{M_{i+1}} \end{cases} \quad i = 1, 2, \dots \quad (9)$$

where t_{M_i} ($i = 1, 2, \dots$) are the time instants at which $\dot{x} = 0$. Note that, in Fig. 2, the 2-SM speed and current controllers are followed by integrators (“antichattering” 2-SMC, [18]); thus, in the suggested scheme, i_r^* and v are *continuous* signals with *discontinuous* time derivative.

Theorem 1 summarizes the overall observer/controller scheme shown in Fig. 2 and establishes sufficient tuning conditions for the three scalar constant tuning parameters U_1, U_2, U_3 , guaranteeing the ultimate boundedness of the speed-tracking error $\omega_r - \omega$.

Theorem 1: Consider system (1), satisfying (2)–(5), and a smooth reference profile ω_r satisfying (6). Set

$$\ddot{z} = \text{SUB}(z - \theta, U_1) \quad (10)$$

$$\frac{d}{dt} i_r^* = \text{SUB}(\dot{z} - \omega_r, U_3) \quad (11)$$

$$\mu \frac{d}{dt} i_r = i_r^* - i_r \quad (12)$$

$$\dot{v} = \text{SUB}(i - i_r, U_2) \quad (13)$$

with the discontinuous function $S(x(t), W)$ defined in (8), initial conditions

$$\begin{aligned} z(0) &= \theta(0) \\ i_r^*(0) &= i_r(0) = i(0) \\ \dot{z}(0) &= v(0) = 0 \end{aligned} \quad (14)$$

and tuning parameters U_1 , U_2 , and U_3 are chosen according to

$$U_1 > 2\Omega_d \tag{15}$$

$$U_2 > 2\Phi_1, \quad \Phi_1 = \frac{2\bar{l}}{\mu}U_3 + \bar{r}I_d + \bar{k}_e\Omega_d \tag{16}$$

$$U_3 > 2\Phi_2, \quad \Phi_2 = \frac{1}{k_t}[\bar{J}\Omega_{\text{rdd}} + \bar{b}\Omega_d + \bar{T}L_d]. \tag{17}$$

Then, there exist finite T , $k > 0$ such that

$$|\omega(t) - \omega_r(t)| \leq k\mu^2, \quad t \geq T. \tag{18}$$

Proof: See the Appendix. ■

Remark 2: Controller tuning.

The tuning of the control parameters U_1 , U_2 , and U_3 is based on inequalities, and it is therefore well suited to be performed in practice by few trial experiments. The U_1 parameter must be set first, at least twice the largest expected acceleration. The U_3 parameter must be then set so as to assign a sufficient bandwidth to the current-loop dynamics. Because of the lag caused by the PWM converter, the tuning of U_3 should be made via trial and error on the real system including the chosen PWM converter. The U_2 parameter has, finally, to be progressively increased until a satisfactory closed-loop performance is observed by using some representative test reference signals such as square waves or sinusoids for the shaft speed and position.

IV. IMPLEMENTATION ISSUES

The digital implementation of the overall scheme is now discussed. Let T_s be the sampling period, and let r_k denote either the k th sample of the analog signal $r(t)$, i.e., $r_k = r(kT_s)$, or the current value of the discrete-time signal r at the k th sampling instant.

The discontinuous function in (8) can be directly discretized as follows [20]:

$$\text{SUB}_d(x_k, W) = -W \text{sign} \left(x_k - \frac{1}{2}x_{Mk} \right) \tag{19}$$

$$x_{Mk} = \begin{cases} x_0, & 0 \leq k < k_{M1} \\ x_{k_{Mi}}, & k_{Mi} \leq k < k_{M,i+1}. \end{cases} \tag{20}$$

The control-signal value $\text{SUB}_d(x_k, W)$ is then used in the k th sampling interval $t \in [kT_s, (k+1)T_s)$ (zeroth-order hold reconstruction method). The sequence k_{Mi} ($i = 1, 2, \dots$) can be computed according to the following algorithm [20]:

$$\begin{aligned} x_{-1} = x_{-2} = x_0, \quad k_{M0} = 0, \quad i = 0, \quad N > 0 \\ \Delta_k = (x_k - x_{k-N})(x_{k-N} - x_{k-2N}) \\ \text{if } \Delta_k < 0 \text{ then } \{i = i + 1, \quad k_{Mi} = k\}. \end{aligned} \tag{21}$$

In the algorithm (21), the measurement delay N is an integer constant to be selected in such a way that the *signs* of the differences $(x_k - x_{k-N})$ and $(x_{k-N} - x_{k-2N})$ are not affected by the measurement noise corrupting the sampled sequence x_k . An appropriate choice of N , whose value should be kept as small as possible, should be made by means of preliminary tests

performed on the actual control system. If the signal x would be noise-free, then the choice $N = 1$ could be made.

The speed observer (10) is implemented as follows [21] by standard zeroth-order hold (ZOH) discretization of the controlled double integrator (10) defining the observer dynamics:

$$\begin{cases} z_{10} = \theta_0; \quad z_{20} = 0 \\ z_{1,k+1} = z_{1k} + z_{2k} T_s + \frac{1}{2} T_s^2 \text{SUB}_d(z_{1k} - \theta_k, U_1) \\ z_{2,k+1} = z_{2k} + T_s \cdot \text{SUB}_d(z_{1k} - \theta_k, U_1) \end{cases} \tag{22}$$

where $z_{2k} = \hat{\omega}_k$ is the output speed estimate.

The remaining part of the control system is also discretized by ZOH method as follows:

$$i_{r0}^* = i_{r0} = i_0, \quad v_0 = 0 \tag{23}$$

$$i_{r,k+1}^* = i_{r,k}^* + T_s \cdot \text{SUB}_d(z_{2k} - \omega_{rk}, U_3) \tag{24}$$

$$i_{r,k+1} = e^{-\frac{T_s}{\mu}} i_{rk} + \left(1 - e^{-\frac{T_s}{\mu}} \right) i_{rk}^* \tag{25}$$

$$v_{k+1} = v_k + T_s \cdot \text{SUB}_d(i_k - i_{rk}, U_2). \tag{26}$$

A detailed stability analysis of the discretized control system would involve similar considerations as those given in [20] and [21] and is skipped for brevity.

A. Accuracy of Digital Implementation

It was shown in [21] that the velocity observer provides a velocity estimate whose error is mainly affected by the sampling effects and by the measurement noise caused by the finite encoder resolution, which leads to a maximal error $\eta = 2\pi/N_p$ (N_p is the number of encoder pulses per revolution).

Provided that the encoder-resolution parameter η is sufficiently small with respect to the actual sampling period T_s , it was shown in [21] that there can be found two constants k_1 , k_2 , independent of T_s and η , such that the estimated velocity $\hat{\omega}$ fulfills the following inequality after a finite transient:

$$|\hat{\omega}(t) - \omega(t)| \leq \max\{k_1 T_s, k_2 \sqrt{\eta}\}. \tag{27}$$

The evaluation of the overall accuracy of the digital control system is a complicated task, since several factors strongly interact in determining it: 1) The measurement error caused by the finite encoder resolution, and its propagation/amplification through the control system; 2) the discretization and quantization of both the measurements and the control signals; and 3) the (intentionally introduced) “parasitic” time constant μ .

Thus, a rigorous analysis of the overall accuracy would require a complex merging of the analysis made in [21] (accuracy of the digital differentiator), [20] (accuracy of the digital realization of the Suboptimal algorithm), and [22] (accuracy in the presence of fast parasitic dynamics).

The exact evaluation of a steady-state upper bound $|\omega(t) - \omega_r(t)|$ would give rise to a complex function of η , T_s , and μ having little practical relevance. Here, we limit ourselves to stress that the combined effect of the earlier three “error” factors will preserve the stability of the closed-loop system as long as the encoder resolution η is sufficiently small with respect to the chosen sampling period T_s and, at the same time, the adopted

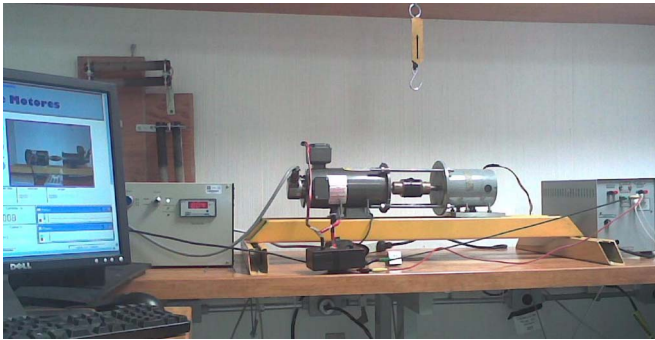


Fig. 3. Experimental setup. Left motor is the master; right motor is the slave.

TABLE I
MASTER MOTOR-DRIVE PARAMETERS AND RATINGS

Back EMF at rated speed	90V
Rating current	2.5A
Torque constant	k_t 0.37NA ⁻¹
Back EMF constant	k_e 0.37Vsrad ⁻¹
Inertia	J_1 0.011kgm ²
Viscous damping coefficient	b 0.0005Ns
Terminal resistance	r 3.565Ω
Leakage inductance	l 37μH

TABLE II
SETUP AND CONTROLLER PARAMETERS

Encoder resolution	N_p	1024 ppr
Bus Voltage		90 V.
PWM frequency		15 kHz
Sampling step	T_s	100μs
Differentiator gain	U_1	200
Speed loop gain	U_2	90
Current loop gain	U_3	90
Smoothing filter time constant	μ	0.01s
Position reference c constant	c	14
Delay in algorithm (21)	N	5

sampling time is sufficiently small with respect to the parasitic time constant μ .

Under the earlier conditions, it can be claimed that, by using the proposed digital controller, there are three constants k_3, k_4, k_5 and a finite transient time T such that

$$|\omega(t) - \omega_r(t)| \leq \max\{k_3 T_s, k_4 \sqrt{\eta}, k_5 \mu^2\}, \quad t \geq T \tag{28}$$

where the constants $k_3, k_4,$ and k_5 independent of $T_s, \eta,$ and μ . In light of (28), it appears appropriate to select μ of order (i.e., comparable with) $\sqrt{T_s}$.

V. EXPERIMENTAL RESULTS

The proposed digital controller (19)–(26) has been implemented on a DSpace DS1104 DSP board. The experimental setup is shown in Fig. 3. Two dc motors are mechanically coupled. One (the master) is velocity controlled using the proposed scheme. The second (the slave) is torque controlled in order to test the control performance against abrupt variations of the load torque. Parameters and ratings of the master PM dc motor are given in the following (Table I).

The main parameters of the experimental setup, and the controller parameters, are reported in Table II.

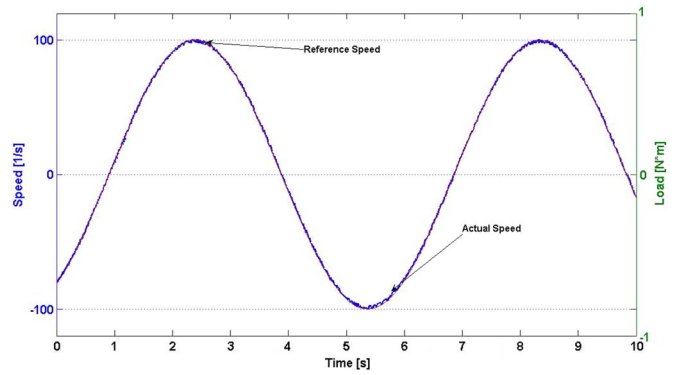


Fig. 4. Actual and reference speeds in TEST 1.

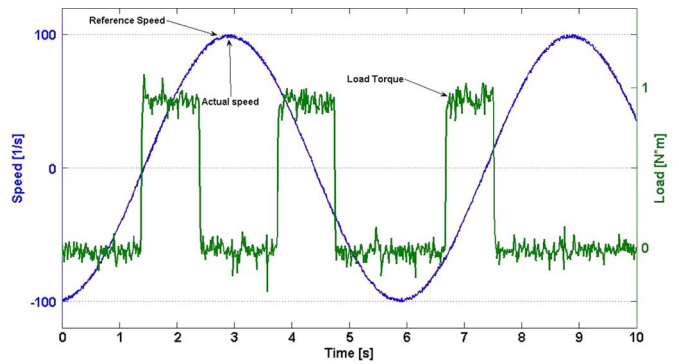


Fig. 5. Load torque and the actual and reference velocities in TEST 2.

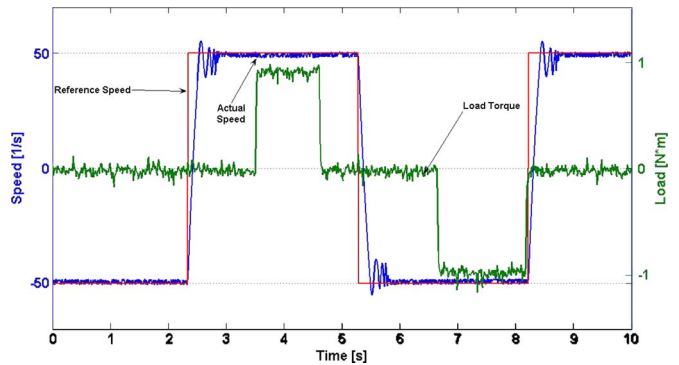


Fig. 6. Load torque and the actual and reference velocities in TEST 3.

Speed- and position-tracking experiments are considered. In all experiments, the controller parameters are kept constant to the values in Table II. In TEST 1, a sinusoidal reference velocity profile $\omega_r = 100 \sin(0.16t)$ rad/s is considered with the slave motor being switched off (no load torque is applied). The actual and reference speeds are shown in Fig. 4.

In TEST 2, the same experiments is repeated with the slave motor switched on and controlled in order to exert a square-wave load torque on the shaft of the master motor. Fig. 5 shows the applied load torque (T_r) and the actual and reference velocities (T_r 2 and T_r 3). It is shown that the step changes in the load torque have no visible effects on the tracking accuracy.

In TEST 3, a square-wave velocity profile switching between the values ± 50 rad/s was considered together with a square-wave load torque applied by the slave motor like in TEST 2. The obtained results are shown in Fig. 6. It can be verified

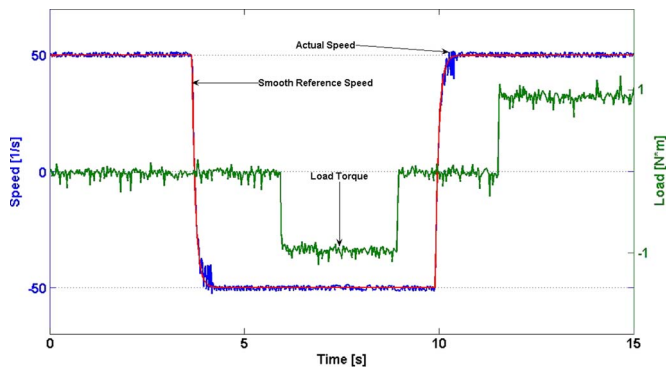


Fig. 7. Applied load torque and the actual and reference velocities in TEST 4.

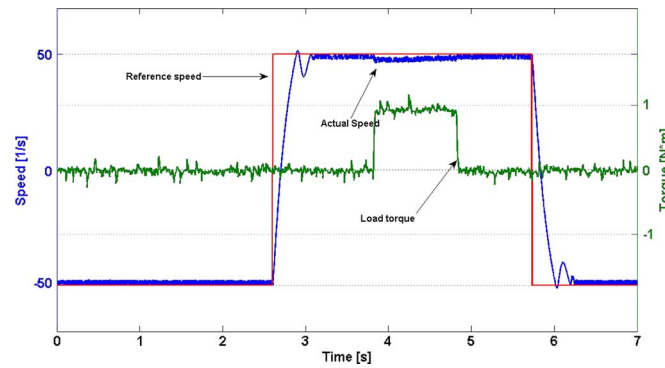


Fig. 9. Applied load torque (Tr. 1) and the actual and reference velocities (Tr. 2 and Tr. 3) in TEST 6 with the PI-based control.

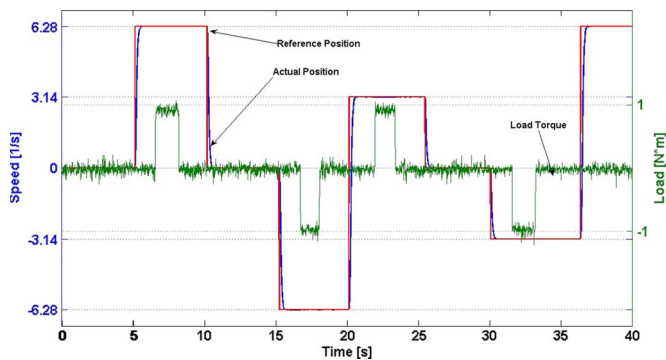


Fig. 8. Applied load torque (Tr. 1) and the actual and reference positions (Tr. 2 and Tr. 3) in TEST 5.

also in this case that the step changes in the load torque have no visible effects on the tracking accuracy. The 2-SMC appears to be very robust. Looking at Fig. 6, the speed transient caused by the changes in the reference appears to be not completely satisfactory due to the overshoot followed by not well-damped oscillations. This phenomenon is caused by the inevitable loss of the SM behavior against the step changes of the reference, which is an “unfeasible” requirement for the motor. Performance can be improved significantly by adopting a continuous reference profile which is a smoothed version of the discontinuous one previously used. This is done in TEST 4, whose results are shown in Fig. 7. The “real” SM behavior is never lost, and it is apparent that, as a direct consequence, using the new smooth profile, the overshoot disappears, and the transient oscillations are attenuated.

In the successive series of tests, *position-regulation problems* are studied. In TEST 5, a piecewise-constant position profile switching between the positions zero and $\pm\pi rad$ is considered. The same previously used piecewise constant-load disturbance is applied through the slave motor. The results are shown in Fig. 8.

A comparison with the performance of a conventional linear PI-based cascade controller has been made as the final test, by considering the same velocity profile as that in TEST 3. The experiment with the PI controller is called TEST 6, whose results are shown in Fig. 9. For a significant comparison, the same 2-SMC algorithm to estimate the shaft velocity has been used also in the PI-based control setup. The parameters of the PIs were selected as follows (by trial and error) for the current

and velocity loops: current loop: $K_p = 210$ and $K_I = 0.4$; velocity loop: $K_p = 220$ and $K_I = 0.5$. As performance-evaluation criteria, consider the maximal deviation from zero of the velocity error after the step change in the applied load torque. It is apparent from the inspection of Fig. 9 that, with the PI control, the actual velocity actually deviates by more than $3 rad^{-1}$, while the 2-SMC scheme (see Fig. 7) is almost insensitive against such an abrupt load change. The higher sensitivity of the linear control scheme against the load variations, as compared with the 2-SM-based one, is therefore highlighted by this test.

VI. CONCLUSION

A new nonlinear control scheme for PM dc motor drives has been proposed, based on the cascade implementation of 2-SM controllers. The proposed solution can be considered as a rather direct generalization of the conventional PI-based cascade-control scheme; every PI controller being replaced by the discontinuous “suboptimal” 2-SMC algorithm followed by an integrator (“chattering-free 2-SMC” [18]). In contrast to the PI-based control, the tuning of the proposed scheme is simpler, since the current and velocity loops are defined by a single scalar parameter to be tuned by means of a simple inequality. The complex adjustment of the proportional and integral gains is avoided, and the tuning can be done, in practice, by few experimental/simulation trials where the controller gains are progressively increased according to the procedure described in the Remark 2. The shaft velocity is estimated by means of the encoder-position measurements via using a real-time differentiator based on the same 2-SMC algorithm. The experimental results have shown the robust performance of the suggested scheme and, in particular, have and put into evidence the superior robustness of the 2-SMC-based control with respect to the conventional PI-based linear control, at least when step changes of the load torque are applied to the motor.

APPENDIX

A. Suboptimal 2-SMC Algorithm

Consider the second-order dynamics

$$\ddot{x} = \gamma [f(t) + u] \tag{29}$$

where $x \in R$ is a measurable signal, $u \in R$ is the control quantity, γ is an unknown positive constant, and $f(t) \in R$ is an uncertain term satisfying

$$|f(t)| \leq F. \tag{30}$$

Define the discontinuous function $\text{SUB}(x(t), W)$ according to (8). The following Lemma is proven.

Lemma 1 [19]: Given system (29) and (30), then the application of the following control law:

$$u = \text{SUB}(x(t), W_1) \tag{31}$$

with the magnitude parameter W_1 satisfying

$$W_1 > 2F \tag{32}$$

provides for the finite-time attainment of the conditions $x = \dot{x} = 0$.

Control algorithm (31) and (32) is referred to as the ‘‘suboptimal’’ 2-SMC algorithm [19].

B. Suboptimal 2-SMC Algorithm With Unmodeled Actuator Dynamics

Analysis of the second-order system (29) cascaded by a dynamic first-order actuator driven by the suboptimal controller has been dealt with in [22]. More precisely, the stabilization problem for the following singularly perturbed second-order dynamics was studied in [22]:

$$\begin{aligned} \ddot{x} &= \gamma [f(t) + u], & |f(t)| &\leq F \\ \dot{u} &= \frac{1}{\mu}(q - u) \end{aligned} \tag{33}$$

with $\mu > 0$ and $q(t) \in R$.

Lemma 2 [22]: Given system (33), then the application of the control law $q = \text{SUB}(x(t), W_1)$, with $W_1 > 2F$, provides for the finite-time attainment of the following conditions:

$$|x| \leq \kappa_1 \mu^2, \quad |\dot{x}| \leq \kappa_2 \mu \tag{34}$$

where κ_1 and κ_2 are constants independent of μ .

Proof of Theorem 1: Define

$$\varepsilon_1 = z - \theta \tag{35}$$

$$\varepsilon_2 = i - \dot{i}_r \tag{36}$$

$$\varepsilon_3 = \omega_r - \dot{z}. \tag{37}$$

Differentiating twice ε_1 , and considering (10), yields

$$\ddot{\varepsilon}_1 = \ddot{z} - \dot{\omega} = \text{SUB}(\varepsilon_1, U_1) - \dot{\omega}. \tag{38}$$

Dynamics (38) is formally equivalent to (29), with $\gamma = 1$, $f = -\dot{\omega}$ (thus, we have that $|f| \leq F = \Omega_d$) and $u = \text{SUB}(\varepsilon_1, U_1)$. Hence, by Lemma 1, if U_1 is set according to condition (15) then both ε_1 and its derivative $\dot{\varepsilon}_1$ are steered to zero in finite time T_1 , i.e.,

$$\varepsilon_1(t) = \dot{\varepsilon}_1(t) = 0, \quad t \geq T_1. \tag{39}$$

This means that $\dot{z} = \omega$; thus, we have that

$$\varepsilon_3(t) = \omega_r(t) - \omega(t), \quad t \geq T_1. \tag{40}$$

Differentiating twice ε_2 , one obtains

$$\begin{aligned} \ddot{\varepsilon}_2(t) &= -\frac{1}{l} \left[\frac{l}{\mu} \left(\text{SUB}(\varepsilon, U_3) - \frac{1}{\mu} (i_r^* - i_r) \right) \right. \\ &\quad \left. + r \frac{d}{dt} i(t) + k_e \frac{d}{dt} \omega(t) - \dot{v}(t) \right] \end{aligned} \tag{41}$$

which can be rewritten as

$$\ddot{\varepsilon}_2(t) = \frac{1}{l} [\varphi_1(t) + \dot{v}(t)] = \frac{1}{l} [\varphi_1(t) + \text{SUB}(\varepsilon_2, U_2)] \tag{42}$$

with

$$\varphi_1(t) = -\frac{l}{\mu} \left[\text{SUB}(\varepsilon_3, U_3) - \frac{1}{\mu} (i_r^* - i_r) \right] - r \frac{d}{dt} i - k_e \frac{d}{dt} \omega. \tag{43}$$

The dynamics (42) is formally equivalent to (29) and (31), then Lemma 1 applies to its analysis. An upper bound to $|\varphi_1(t)|$ is now evaluated, since it is needed in order to properly find out the tuning condition on the U_2 parameter which guarantees the finite-time zeroing of $\varepsilon_2(t)$ and $\dot{\varepsilon}_2(t)$. Define the variable

$$\xi = i_r^* - i_r \tag{44}$$

and consider the Lyapunov function

$$V = \frac{1}{2} \xi^2 \tag{45}$$

whose time derivative along the trajectory of (12) is given by

$$\begin{aligned} \dot{V} &= - \left[\frac{1}{\mu} \xi - \frac{d}{dt} i_r^*(t) \right] \xi \\ &= - \left[\frac{1}{\mu} |\xi| - \frac{d}{dt} i_r^*(t) \text{sign}(\xi) \right] |\xi|. \end{aligned} \tag{46}$$

By (8) and (11), it follows that

$$\left| \frac{d}{dt} i_r^*(t) \text{sign}(\xi) \right| = U_3. \tag{47}$$

Considering (46) and (47), it follows by standard Lyapunov analysis that the following domain:

$$|\xi| < \mu U_3 \tag{48}$$

inside which the time derivative of V is negative definite, is invariant. Since $\xi(0) = 0$, then condition (48) holds from $t = 0$ on. In the light of (48), and considering (4) and (5) into (43), the term $\varphi_1(t)$ can be finally bounded as follows:

$$|\varphi_1| \leq \Phi_1, \quad \Phi_1 = \Phi_1 = \frac{2\bar{l}}{\mu} U_3 + \bar{r} I_d + \bar{k}_e \Omega_d, \quad t \geq T_1. \tag{49}$$

If parameter U_2 is set according to (16), i.e., greater than two times the earlier computed bound Φ_1 , then both ε_2 and its derivative $\dot{\varepsilon}_2$ are steered to zero in a finite time $T_2 > T_1$, i.e.,

$$\varepsilon_2(t) = \dot{\varepsilon}_2(t) = 0, \quad t \geq T_2. \quad (50)$$

Differentiating twice ε_3 and performing some algebraic manipulations yields

$$\ddot{\varepsilon}_3(t) = \frac{k_t}{J} \left[\frac{J}{k_t} \ddot{\omega}_r + \frac{b}{k_t} \dot{\omega} + \frac{1}{k_t} \dot{T}_l(t) - \frac{d}{dt} i \right]. \quad (51)$$

By (36) and (50), condition $i = i_r$ holds, and the right-hand side of (51) can be rewritten as follows:

$$\ddot{\varepsilon}_3(t) = \frac{k_t}{J} \left[\frac{J}{k_t} \ddot{\omega}_r + \frac{b}{k_t} \dot{\omega} + \frac{1}{k_t} \dot{T}_l(t) - \frac{d}{dt} i_r \right], \quad t \geq T_2. \quad (52)$$

Now, let

$$\beta = -\frac{d}{dt} i_r \quad (53)$$

$$\varphi_2 = \frac{1}{k_t} \left[J\ddot{\omega}_r + b\dot{\omega} + \dot{T}_l(t) \right]. \quad (54)$$

As soon as the 2-SM condition (50) has been established at $t \geq T_2$, the coupled dynamics (12) and (52) can be rewritten as

$$\begin{aligned} \ddot{\varepsilon}_3(t) &= \frac{k_t}{J} [\varphi_2 + \beta] \\ \mu\dot{\beta} + \beta &= \text{SUB}(\varepsilon_3, U_3) \end{aligned} \quad (55)$$

with φ_2 bounded as follows:

$$|\varphi_2| \leq \Phi_2, \quad \Phi_2 = \frac{1}{k_t} \left[\bar{J}\Omega_{rdd} + \bar{b}\Omega_d + \bar{T}_{Ld} \right], \quad t \geq T_2. \quad (56)$$

Systems (55) and (56) can be analyzed by Lemma 2; hence, if U_3 satisfies the tuning inequality (17), then ε_3 enters in finite time $T_3 > T_2$ an invariant set of the type

$$|\varepsilon_3(t)| = \rho\mu^2, \quad t \geq T_3 \quad (57)$$

for some $\rho > 0$ independent of μ , which is equivalent to condition (18), thus proving the Theorem. ■

REFERENCES

[1] W. Leonhard, *Control of Electric Drives*. London, U.K.: Springer-Verlag, 1985.
 [2] C. Attaianesi, A. Peretto, and G. Tomasso, "Robust position control of DC drives by means of H_∞ controllers," *Proc. Inst. Elect. Eng.—Elect. Power Appl.*, vol. 146, no. 4, pp. 391–396, Jul. 1999.
 [3] H. Butler, G. Honderd, and J. van Amerongen, "Model reference adaptive control of a direct-drive DC motor," *IEEE Control Syst. Mag.*, vol. 9, no. 1, pp. 80–84, Jan. 1989.

[4] P. Dobra, "Robust PI control for servo DC motors," in *Proc. IEEE Int. Conf. Control Appl.*, 2002, pp. 100–101.
 [5] K. Ohishi *et al.*, "Microprocessor-controlled DC motor for load-insensitive position servo systems," *IEEE Trans. Ind. Electron.*, vol. IE-34, no. 1, pp. 44–49, Feb. 1987.
 [6] J. O. Jang, "Neural network saturation compensation for DC motor systems," *IEEE Trans. Ind. Electron.*, vol. 54, no. 3, pp. 1763–1767, Jun. 2007.
 [7] T. L. Chern and J. S. Wong, "DSP based integral variable structure control for DC motor servo drives," *Proc. Inst. Elect. Eng.—Control Theory Appl.*, vol. 142, no. 5, pp. 444–450, Sep. 1995.
 [8] V. I. Utkin, J. Gulder, and J. Shi, *Sliding Mode Control in Electromechanical Systems*. London, U.K.: Taylor & Francis, 1999.
 [9] J. Y. Hung, W. Gao, and J. C. Hung, "Variable structure control: A survey," *IEEE Trans. Ind. Electron.*, vol. 40, no. 1, pp. 2–22, Feb. 1993.
 [10] K. D. Young, V. I. Utkin, and Ü. Özgüner, "A control engineer's guide to sliding mode control," *IEEE Trans. Control Syst. Technol.*, vol. 7, no. 3, pp. 328–341, May 1999.
 [11] A. Sabanovic, K. Jezernik, and N. Sabanovic, "Sliding modes applications in power electronics and electrical drives," in *Variable Structure Systems: Towards the 21st Century*, vol. 274, X. Yu and J.-X. Xu, Eds. Berlin, Germany: Springer-Verlag, 2002, pp. 223–251.
 [12] V. I. Utkin, "Sliding modes control design principles and applications to electric drives," *IEEE Trans. Ind. Electron.*, vol. 40, no. 1, pp. 23–35, Feb. 1993.
 [13] Z. Yan, C. Jin, and V. I. Utkin, "Sensorless sliding-mode control of induction motors," *IEEE Trans. Ind. Electron.*, vol. 47, no. 6, pp. 1286–1297, Dec. 2000.
 [14] K. Abidi and A. Sabanovic, "Sliding-mode control for high-precision motion of a Piezostage," *IEEE Trans. Ind. Electron.*, vol. 54, no. 1, pp. 629–637, Feb. 2007.
 [15] C. Rossi and A. Tonielli, "Robust control of permanent magnet motors: VSS techniques lead to simple hardware implementations," *IEEE Trans. Ind. Appl.*, vol. 41, no. 4, pp. 451–460, Aug. 1994.
 [16] F. J. Chang, S. H. Twu, and S. Chang, "Tracking control of DC motors via an improved chattering alleviation control," *IEEE Trans. Ind. Electron.*, vol. 39, no. 1, pp. 25–29, Feb. 1992.
 [17] J. Zhang and T. Barton, "Robustness enhancement of dc drives with a smooth optimal sliding-mode control," *IEEE Trans. Ind. Electron.*, vol. 27, no. 4, pp. 686–693, Jul./Aug. 1991.
 [18] G. Bartolini, A. Ferrara, and E. Usai, "Chattering avoidance by second order sliding mode control," *IEEE Trans. Autom. Control*, vol. AC-43, no. 2, pp. 241–246, Feb. 1998.
 [19] G. Bartolini, A. Ferrara, A. Levant, and E. Usai, "On second order sliding mode controllers," in *Variable Structure Systems, Sliding Mode and Nonlinear Control*, vol. 247, K. D. Young and U. Ozguner, Eds. Berlin, Germany: Springer-Verlag, 1999, pp. 329–350.
 [20] G. Bartolini, A. Pisano, and E. Usai, "Variable structure control of nonlinear sampled data systems by second order sliding modes," in *Variable Structure Systems, Sliding Mode and Nonlinear Control*, vol. 247, K. D. Young and U. Ozguner, Eds. Berlin, Germany: Springer-Verlag, 1999, pp. 44–67.
 [21] G. Bartolini, A. Damiano, G. Gatto, I. Marongiu, A. Pisano, and E. Usai, "Robust speed and torque estimation in electrical drives by second order sliding modes," *IEEE Trans. Control Syst. Technol.*, vol. 11, no. 1, pp. 84–90, Jan. 2003.
 [22] I. Boiko, L. Fridman, A. Pisano, and E. Usai, "Analysis of chattering in systems with second-order sliding-mode," *IEEE Trans. Autom. Control*, vol. 52, no. 11, pp. 2085–2102, Nov. 2007.
 [23] A. Levant, "Sliding order and sliding accuracy in sliding mode control," *Int. J. Control*, vol. 58, no. 6, pp. 1247–1263, 1993.
 [24] A. Damiano, G. Gatto, A. Pisano, and E. Usai, "Digital second order sliding mode control of PM DC motor," in *Proc. ISIE*, Bled, Slovenia, 1999, pp. 322–326.
 [25] A. Damiano, G. Gatto, I. Marongiu, and A. Pisano, "Second-order sliding-mode control of DC drives," *IEEE Trans. Ind. Electron.*, vol. 51, no. 2, pp. 364–373, Apr. 2004.
 [26] M. Khalid Khan, C. Edwards, and S. K. Spurgeon, "Second order sliding mode control applied to DC motor position control with limited state availability," in *Proc. 8th IEEE Int. Workshop Variable Structure Systems (VSS'04)*, Vilanova i la Geltru, Spain, Sep. 6–8, 2004, Paper 24.
 [27] A. Levant, "Higher-order sliding modes, differentiation and output-feedback control," *Int. J. Control*, vol. 76, no. 9/10, pp. 924–941, Jun. 2003.



Alessandro Pisano (M'07) was born in Sassari, Italy, in 1972. He received the M.S. (Laurea) degree in electronic engineering and the Ph.D. degree in electronics and computer science from the Department of Electrical and Electronic Engineering (DIEE), Cagliari University, Cagliari, Italy, in 1997 and 2000, respectively.

He is currently a Research Associate with DIEE, Cagliari University. His current research interest includes the theory and application of nonlinear and robust control, with special emphasis on sliding-mode control design and implementation, robotics, and power-plant simulation and control. He is Co-Editor of the book *Modern Sliding Mode Control Theory—New Perspectives and Applications* (Springer Lecture Notes in Control and Information Sciences, vol. 375, 2008) and has authored over 80 journal and conference papers. He is the holder of two patents in the field of underwater robotics and industrial control systems.

Dr. Pisano is a Professional Engineer registered in Cagliari. He served as the Chair of the National Organizing Committee and a Program Committee Member for the 9th IEEE International Workshop on Variable Structure Systems (VSS 2006). He is an Associate Editor of the Conference Editorial Board, IEEE Control Systems Society.



Alejandro Davila was born in Queretaro, Mexico, in 1980. He received the B.S. degree in electrical and electronic engineering from the National Autonomous University of Mexico, Mexico City, Mexico, in 2006, where he is currently working toward the M.S. degree in electrical-control engineering.

His research interests include nonlinear robust control with sliding modes as applied to electric drives.



Leonid Fridman (M'96) received the M.S. degree in mathematics from Kuibyshev (Samara) State University, Samara Oblast, Russia, in 1976, the Ph.D. degree in applied mathematics from the Institute of Control Science, Moscow, Russia, in 1988, and the Dr. of Science degree in control science from Moscow State University of Mathematics and Electronics, Moscow, in 1998.

From 1976 to 1999, he was with the Department of Mathematics, Samara State Architecture and Civil Engineering Academy, Samara, Russia. From 2000 to 2002, he was with the Department of Postgraduate Study and Investigations, Chihuahua Institute of Technology, Chihuahua, Mexico. Since 2002, he has been with the Department of Control, Division of Electrical Engineering of Engineering Faculty, National Autonomous University of Mexico, Mexico City, Mexico. He is an Editor of two books and four international journal Special Issues on sliding-mode control. He published over 160 technical papers. His research interests include variable-structure systems and singular perturbations.

Dr. Fridman is an Associate Editor of the Conference Editorial Board, IEEE Control Systems Society, and a Member of the Technical Committee on Variable Structure Systems and Sliding-mode Control, IEEE Control Systems Society.



Elio Usai (M'97) was born in Sassari, Italy, in 1960. He received the M.S. (Laurea) degree in electrical engineering from the University of Cagliari, Cagliari, Italy, in 1985.

Until 1994, he was working for international industrial companies. Since 1994, he has been with the Department of Electrical and Electronic Engineering, University of Cagliari, where he is currently an Associate Professor of automatic control. His current research interests are in the field of control engineering, variable-structure systems, and control

of mechanical systems.